



# Effects of brown coatings on the absorption enhancement of black carbon: a numerical investigation

Jie Luo, Yongming Zhang, Feng Wang, and Qixing Zhang

State Key Laboratory of Fire Science, University of Science and Technology of China, Hefei, Anhui 230026, China

**Correspondence:** Qixing Zhang (qixing@ustc.edu.cn)

**Abstract.** Using the numerically exact multiple sphere T-matrix (MSTM) method, we explored the effects of brown coatings on absorption enhancement ( $E_{abs}$ ) and the lensing effects ( $E_{abs\_lensing}$ ) of black carbon (BC) at different wavelengths ( $\lambda$ ).  $E_{abs}$  increases with the absorption of coatings, while an opposite trend is observed for  $E_{abs\_lensing}$ . A much wider range of  $E_{abs}$  is observed for BC with brown coatings compared to that with non-absorbing coatings.  $E_{abs}$  can reach approximately 5.4 for  $\lambda = 0.35 \text{ } \mu\text{m}$  given a typical size distribution. In addition, previous studies have focused on the lensing effects of coatings but neglected the blocking effects of absorbing coatings.  $E_{abs\_lensing}$  can be below 0.5 at ultraviolet spectral region for BC with brown coatings, which indicates that the absorption of internal BC is diluted by approximately 0.5 times due to the blocking effects of outer coatings, and we named the blocking effect of absorbing coatings "sunglasses effect". Hence, it is imperative to take the blocking effects of outer coatings into consideration for estimation of total aerosol absorption.  $C_{abs}$  of thickly-coated BC is underestimated by core-shell sphere model for all wavelengths while the underestimation becomes negligible as  $k_{BC}$  turns very large.  $E_{abs}$  and  $E_{abs\_lensing}$  are insensitive to the size distribution for thinly-coated BC, and the uncertainties caused by the size distribution have differences of less than 2.6% and 6%, respectively. However, the effects of size distribution on  $E_{abs}$  and  $E_{abs\_lensing}$  are rather obvious for thickly-coated BC. In addition, the uncertainties in  $E_{abs}$  and  $E_{abs\_lensing}$  caused by  $D_f$  are less than 9%.  $E_{abs}$  seems to be essentially wavelength-independent for thickly-coated BC with non-absorbing coatings but rather wavelength-dependent for thickly-coated BC with brown coatings.

## 1 Introduction

Recent modeling and field studies have indicated that aerosol light absorption is an important contributor to climate forcing (Jacobson, 2001; Krishnan and Ramanathan, 2002). Black carbon (BC), which is a product of incomplete combustion, is the strongest solar-absorbing aerosol in the atmosphere (Lack et al., 2009; Zhang et al., 2008). BC radiative forcing from fossil fuels and biomass burning have been estimated to be approximately  $0.4 \text{ W/m}^2$ , as the second contribution (after  $\text{CO}_2$ ) to climate forcing due to their strong absorption of solar radiation (Forster et al., 2007; Schwarz et al., 2008). Sensitivity tests suggest that the mixing state and morphology of BC aerosols can largely affect the absorption of BC (Ma et al., 2012; Zhang et al., 2018). Due to the large uncertainties of BC morphologies and mixing states, the understanding of BC absorption is still limited. Even when coated with non-absorbing materials, the BC absorption can be enhanced (Liu et al., 2017; Cappa et al.,



2012). Many studies mainly attribute the absorption enhancements ( $E_{abs}$ ) to the lensing effect (Bond et al., 2006; Fuller et al., 1999).

For the estimation of BC absorption enhancements, many field measurements have been conducted. Naoe et al. (2009) presented factors of 1.1-1.4 for BC absorption enhancement at a suburban site in Japan, while Cui et al. (2016) indicated that the absorption enhancement factors increase from  $1.4 \pm 0.3$  during fresh combustions to  $\sim 3$  for aged BC in a rural site over the North China Plain (NCP). Liu et al. (2017) found that BC absorption enhancement is significantly influenced by the particle mixing state. The measured range of  $E_{abs}$  is approximately  $1 \sim 1.5$ . You et al. (2016) observed the wavelength-dependent absorption enhancement of coated BC. In their measurements,  $E_{abs}$  increased up to 3 at the shortest measured wavelengths, while it was approximately 1.6 in the near-IR wavelength. A negligible absorption enhancement of only 6% for ambient BC particles was reported by Cappa et al. (2012) based on direct measurements over California (USA). Chen et al. (2017) reported an average  $E_{abs}$  of  $2.07 \pm 0.72$  for the urban haze in winter in northern China. However, this result was time-dependent. The absorption enhancement of BC during the urban PM<sub>2.5</sub> pollution was  $1.31 \pm 0.29$  in the morning, while in the afternoon, it increased to approximately  $2.23 \pm 1.05$ ; then, it decreased to  $1.52 \pm 0.75$  in the evening. In summary, the reported  $E_{abs}$  values are not consistent in different studies due to the complex aging statuses.

Although the field measurements can provide referential absorption enhancement values for different aging statuses and regions, causes of these enhancements are not clear. For example, what is the main factor that causes the complex absorption enhancements: morphology, the mixing states or the types of coatings? To our best knowledge, field measurements have difficulty answering these questions currently. Numerical simulation is a strong tool that reveals the mechanism responsible for the complex absorption enhancements. To improve the understanding of the complex absorption enhancements of BC, numerical studies have also been conducted. For instance, based on the core-shell Mie theory, the absorption enhancement factors have been estimated up to 3 (Bond et al., 2006). By the numerically exact multiple sphere T-matrix (MSTM) method, Zhang et al. (2017) presented the absorption enhancements of non-absorbing coatings for aged BC ranging from 1.1-2.4, and they were significantly influenced by the morphology and aging statuses but insensitive to the BC refractive index. However, previous studies have failed to uncover the effects of coating absorption. In their studies, coatings were considered as non-absorbent, and BC absorption enhancements were completely caused by lensing effects. Nevertheless, in the atmosphere, there is a type of organic carbon that absorbs the radiation in the range of the ultraviolet and visible spectra, which is known well as brown carbon (BrC); BC can also be mixed with BrC. Compared with non-absorbing OC, the absorption of BrC is significantly wavelength-dependent, and the imaginary part of the refractive index for BrC has a wide range (Kirchstetter et al., 2004), which results in large uncertainties for the estimation of aerosol absorption. Therefore, the absorption of BrC has gained increasing interests (Kirchstetter et al., 2004; Shamjad et al., 2018).

Many studies have been conducted to evaluate the absorption of BrC. One typical method for the determination of BrC absorption is isolating BrC by extracting filtered samples (Cheng et al., 2017). This method can be used to determine the imaginary part of the BrC refractive index. However, it is difficult to understand the effects of BrC on the total aerosol absorption, as BrC is commonly mixed with other chemical compositions. The assumption of externally mixing can be used to evaluate the absorption of BrC and BC separately. Nevertheless, in many cases, BC is internally mixed with other materials. It is widely



accepted that the absorption is underestimated by the external mixing assumption when BC is coated with non-absorbing materials due to lensing effects. However, whether this is true for BC with BrC coatings is not clear. To understand the effects of BrC coatings, the contributions of "lensing effects" and the total absorption enhancement of BC with BrC coatings should be analyzed individually.

- 5 Cheng et al. (2017) has conducted a numerical investigation on BC absorption enhancement, BrC absorption enhancement and lensing effects on BC mixed BrC by assuming a core-shell structure. While the internal mixing of BC is widely accepted, the core-shell structure is debated (Adachi et al., 2010; Cappa et al., 2012; Bond et al., 2013). He et al. (2015) developed a theoretical BC aging model and concluded that the evolution of coating thickness, morphology, and composition during the aging process could have significant impacts on BC absorption. To investigate the lensing effects and total absorption  
10 enhancements of BrC coatings throughout the whole aging process, two types of mixing states were considered: thinly-coated BC and thickly-coated BC.

In this study, a numerical investigation was conducted for the evaluation of the lensing effects and the absorption enhancement of BC with BrC coatings for different mixing states. The results would give further understanding for the causes of BC absorption enhancements and suggestion for the inferred BC mixing states.

## 15 2 Methodology

### 2.1 Geometric properties of BC aerosols

In climate modeling, a spherical shape is commonly assumed for aerosols and can be calculated with high efficiency using the Mie theory (Mie, 1908). However, in many cases, this shape can introduce large errors compared with the measurements due to the oversimplification of the shape. Recently, the nonsphericity of aerosols has gained increasing interests (Yang et al., 2003; Bi and Yang, 2016). Specifically, observations have indicated that uncoated BC particles are commonly composed of numerous small spherical particles. Fractal aggregates can be greatly used to describe their geometric properties. Mathematically, the structure satisfies the well-known fractal law (Mishchenko et al., 2002):

$$n_s = k_0 \left( \frac{R_g}{R} \right)^{D_f} \quad (1)$$

$$R_g^2 = \frac{1}{n_s} \sum_{i=1}^{n_s} l_i^2 \quad (2)$$

where  $n_s$  represents the number of the monomers in the cluster,  $R$  represents the mean radius of the monomers,  $k_0$  represents the fractal prefactor,  $D_f$  represents the fractal dimension,  $R_g$  represents the radius of gyration, and  $l_i$  represents the distance from the  $i$ th monomer to the center of the cluster.

- 20 The fractal dimension is a key parameter that describes the compactness of BC aggregates (Sorensen, 2001; Sorensen and Roberts, 1997; Luo et al., 2018a). Generally, aggregates tend to be more compact with the increase in  $D_f$ . A  $D_f$  of 1 can describe an open-chain-type shape, while the aggregates tend to be spherical as  $D_f$  approaches 3. Numerous experimental studies have been carried out to evaluate the  $D_f$  of BC aggregates. Immediately after they are emitted, BC aggregates generally



exhibit fluffy structures with a small fractal dimension ( $D_f$ ), that is normally less than 2, such as the  $D_f$  of BC aggregates from biomass burnings (1.67-1.83) (Chakrabarty et al., 2006), the  $D_f$  of BC from vehicle emissions (1.52-1.94) (China et al., 2014), and the  $D_f$  of BC from diesel (1.6-1.9) (Wentzel et al., 2003).

However, under the effects of atmospheric aging, the structures and chemical compositions of BC may change. Aged BC tends to be mixed with other chemical components, and the shape becomes more compact. Therefore, in the atmosphere, aggregates can have fractal dimensions up to 2.6 (Chakrabarty et al., 2006). In some cases, BC aggregates are thinly coated with other materials, and still exhibit a fractal structure. However, different from freshly emitted BC aggregates, both lacy and compact structures can exist. Therefore, for thinly-coated BC, the  $D_f$  was assumed to be in the range from 1.8 – 2.6. As BC becomes increasingly coated, BC aggregates may transform from highly agglomerated to nearly spherical particles. A  $D_f = 2.6$  was assumed for thickly-coated BC. Even though a fractal prefactor can also vary under different combustion and aging statuses, it has less significant effects on the absorption of BC compared to the  $D_f$ . When fixing  $D_f$  to be 1.82, Liu and Mishchenko (2005) demonstrated that the absorption cross-section of BC aggregates does not change substantially as fractal prefactor varies from 0.9 to 2.1. Therefore, a fixed fractal prefactor of 1.2 was assumed in this work.

The monomer radius and monomers number are two key parameters that determine the particle size. Even though the monomers radii are polydispersed in the atmosphere, they vary within a narrow range. Monomer radii are commonly observed within  $\sim 10$ -25 nm (Bond and Bergstrom, 2006). In addition, Kahnert (2010b) demonstrated that  $C_{abs}$  is insensitive to monomer radii when the monomer radii are within  $\sim 10$ -25 nm. As a result, for convenient application, a fixed monomer radius of  $R = 20$  nm was assumed in this work. Based on TEM/SEM image, the monomer number  $n_s$  can reach approximately 800 (Adachi and Buseck, 2008). Values of  $1 \leq n_s \leq 1000$  were considered in this work. For an aggregate with  $n_s$  monomers, the equivalent radius was given by the equivalent volume sphere radius  $R\sqrt[3]{n_s}$ . The morphological parameters considered in this work are shown in Table 1.

## 2.2 Generation of BC aerosols

The morphologies of coated BC considered in this work are classified into two categories: thinly-coated BC and thickly-coated BC. The closed-cell structure, which is an example of where coating material that not only covers the outer layers of BC aggregates but also fills the internal voids among primary spherules, can be used to represent the thinly-coated BC (Liou et al., 2011; Strawa et al., 1999). In addition, Kahnert (2017) demonstrated that the absorption of closed-cell structures and more realistic morphologies do not have large deviations. Therefore, it is reasonable to use the closed-cell model for calculating the absorption of thinly-coated BC, while the thickly-coated BC are commonly represented by a structure where BC aggregates are encapsulated in a sphere (Zhang et al., 2017; Cheng et al., 2014). The typical morphologies are shown in Fig. 1.

Diffusion-limited algorithms (DLA), including the particle-cluster aggregation (PCA) (Hentschel, 1984) and the cluster-cluster aggregation (CCA) methods (Thouy and Jullien, 1994), have been developed for the generation of aggregates. However, adjustable DLA codes are commonly applied due to its quick implementation and adjustable fractal parameters (Koylu et al., 1995). In this work, an adjustable DLA code developed by Woźniak (2012) was used. Compared with ordinary DLA codes, this code preserves fractal parameters during each step of the aggregation, which avoids the generation of multifractal aggregates



(Jensen et al., 2002). After the generation of the aggregates, the coatings were added. More specifically, for thinly-coated BC, the BrC shells were generated by the adjustable algorithm, and then the BC cores were added; the details are shown in previous studies (Luo et al., 2018c; Wu et al., 2014). The thickly-coated BC is generated by covering the BrC spherical coatings on the BC aggregates, as shown in the study of Cheng et al. (2015).

## 5 2.3 Light scattering method

To calculate the radiative properties of BC in this work, numerical solution methods from Maxwell's equations, including the finite-difference time-domain (FDTD) method (Yee, 1966; Taflove and Hagness, 2005), generalized multiparticle Mie (GMM) method (Xu, 1997; Xu and Gustafson, 2001), numerically exact multiple sphere T-matrix (MSTM) method (Mackowski and Mishchenko, 2011; Mishchenko et al., 2004) and discrete-dipole approximation (DDA) method (Draine and Flatau, 1994; Laczik, 1996; Smith and Stokes, 2006), can all be used. However, compared with other numerical methods, the MSTM has an advantage for the calculation of optical properties for randomly oriented particles analytically without numerically averaging over particle orientations. Therefore, this method has high efficiency to calculate optical properties of BC. In this work, the latest MSTM code, MSTM version 3.0 (Mackowski, 2013), was applied.

## 2.4 Calculating absorption enhancement and lensing effects

The presence of non-BC coated materials can result in the enhancement of BC absorption. However, it is difficult to distinguish how these enhancements are caused (i.e., by "lensing effect" or by the absorption of BrC). Based on Cheng et al. (2017), we attribute the BC absorption enhancements to two factors: (1) the effect of BrC absorption ( $E_{abs\_BrC}$ ); (2) the effects of lensing ( $E_{abs\_lensing}$ ), which indicates that the shell can act as a lens that changes the absorption enhancement. It can be used to evaluate the relation between the absorption of a total particle and the sum of the coating and BC separately. When  $E_{abs\_lensing} > 1$ , the total absorption is enhanced by internally mixing, while the total absorption is weakened when  $E_{abs\_lensing} < 1$ . Here,  $E_{abs\_lensing}$  characterizes the comprehensive outcome of lensing effects and blocking effects caused by coatings. To evaluate the effects of BrC coatings on the absorption enhancement of BC,  $E_{abs}$  and  $E_{abs\_lensing}$  were calculated using:

$$E_{abs} = \frac{C_{abs\_whole\ particle}}{C_{abs\_bare}} \quad (3)$$

$$E_{abs\_BrC} = \frac{C_{abs\_BrC(\ total\ size)} - C_{abs\_BrC(\ bare\ size)}}{C_{abs\_bare}} \quad (4)$$

$$E_{abs\_lensing} = E_{abs} - E_{abs\_BrC} \quad (5)$$

15 where  $C_{abs\_whole\ particle}$  and  $C_{abs\_bare}$  represent the absorption cross-sections of coated BC and bare BC respectively.  $C_{abs\_BrC(\ total\ size)}$  and  $C_{abs\_BrC(\ bare\ size)}$  represent the absorption cross-sections of BrC with morphologies that are identical for coated BC and bare BC, respectively.



## 2.5 Size distribution

The absorption of BC is significantly affected by the particle size (Kahnert, 2010b; Luo et al., 2018b). Therefore, the effects of the size distribution on BC absorption enhancement should be considered carefully. The shape of BC particles is commonly irregular. To describe the size of each BC particle, the radius of the corresponding equivalent volume sphere is typically used. Based on numerous measurements, a lognormal size distribution is observed to fit the realistic BC size distributions well (Bond et al., 2002; Chakrabarty et al., 2006; Wang et al., 2015), and it is widely used in climate models for the estimation of BC radiative forcing (Moffet and Prather, 2009; Chung et al., 2012). However, the mean size and standard deviation vary with the combustion status and aging status. In the atmosphere, geometric mean radii ( $r_g$ ) between 0.05  $\mu\text{m}$  and 0.06  $\mu\text{m}$  for BC are widely accepted (Alexander et al., 2008; Coz and Leck, 2011; Liu et al., 2018; Li et al., 2016). The geometric standard deviation ( $\sigma_g$ ) varies within a relatively narrow range. Consequently, bare BC with an  $r_g$  between 0.03  $\mu\text{m}$  and 0.1  $\mu\text{m}$  is considered for sensitivity analysis, an  $\sigma_g$  varies from 1.15-1.75. The minimum and maximum equivalent volume radii are  $r_{min} = 0.02 \mu\text{m}$  and  $r_{max} = 0.2 \mu\text{m}$ , respectively.

To estimate the effects of coating thickness on the absorption properties of BC, we assumed that BrC coatings are uniformly coated on the BC, and the mixing states are independent of BC size. The difference between the size distributions of bare BC and coated BC is attributed to the coatings thickness. The size distribution of bare and coated BC is shown in Fig. 2. Even though the assumption does not completely agree with the real cases, it is reasonable to make some simplifications to the sensitivity analysis. Here, we must classify that the size distribution parameters ( $r_g$  and  $\sigma_g$ ) mentioned in this work are applied for the bare BC, and the overall effective volume radius of coated BC is equal to the sum of coatings thickness and radius of bare BC.

## 2.6 Calculation of bulk radiative properties of BC

To make our work more consistent with real circumstance, bulk optical properties are considered. These properties are calculated by averaging over a certain particle size distribution. In application, the equivalent volume radii of BC are commonly assumed to follow a lognormal size distribution :

$$n(r) = \frac{1}{\sqrt{2\pi r \ln(\sigma_g)}} \exp \left[ - \left( \frac{\ln(r) - \ln(r_g)}{\sqrt{2 \ln(\sigma_g)}} \right)^2 \right] \quad (6)$$

where  $r_g$  and  $\sigma_g$  represent the geometric mean radius and geometric standard deviation, respectively. Given the size distribution, the bulk  $C_{abs}$  can be obtained by the following equation:

$$\langle C_{abs} \rangle = \int_{r_{min}}^{r_{max}} C_{abs}(r) n(r) dr \quad (7)$$

The bulk  $E_{abs}$ ,  $E_{abs\_BrC}$  and  $E_{abs\_lengsing}$  are similar to those in equations 3-5. The only difference is that the absorption cross-section is now bulk absorption cross-section.





### 3 Results

#### 3.1 Effects of the imaginary part of the BrC refractive index: lensing effect and sunglasses effect

The refractive index of BC is commonly assumed to be wavelength-independent over the visible and near-visible spectral regions, and the imaginary part  $k_{BC} \approx 0.79$  (Moosmuller et al., 2009; Bond and Bergstrom, 2006). In addition, Zhang et al. (2017) has demonstrated that the uncertainties of the BC refractive index have little impact on the absorption enhancement of coated BC aggregates. Therefore, a typical refractive index  $m = 1.95 + 0.79i$  of BC, was adopted in this study.

For BrC, the real parts of the BrC refractive indices were assumed to have a constant value of 1.5 (Schnaiter et al., 2005), while the imaginary part of the refractive index ( $k_{BrC}$ ) was significantly dependent on wavelength at shorter visible and ultraviolet (UV) wavelengths (Moosmuller et al., 2009; Andreae and Gelencser, 2006; Alexander et al., 2008). Fig. 3 shows the effects of  $k_{BrC}$  on  $E_{abs}$  and  $E_{abs\_lensing}$ , where  $f_{BC}$  represents the BC volume fraction. Large deviations in  $E_{abs}$  and  $E_{abs\_lensing}$  can be observed given different values of  $k_{BrC}$ . Generally,  $E_{abs}$  increases with  $k_{BrC}$ , while  $E_{abs\_lensing}$  decreases with increasing  $k_{BrC}$ . Therefore, it is desirable to evaluate the effects of absorbing coatings on BC absorption enhancement. Given identical  $k_{BrC}$  values, the absorption enhancements of thickly-coated BC increases with wavelength. However, for BC that is internally mixed with BrC, wavelength-dependent absorption enhancements are measured to decrease with  $\lambda$  (You et al., 2016). This may be due to the wavelength-dependent  $k_{BrC}$ . For aged BC,  $E_{abs\_lensing}$  and  $E_{abs}$  decrease with wavelength, but they are not a strong function of  $\lambda$  for thinly-coated BC. In addition, compared with BC with non-absorbing coatings,  $E_{abs}$  for thinly-coated BC with absorbing coatings seems to be less wavelength-dependent, while  $E_{abs}$  for thickly-coated BC with absorbing materials is more sensitive to wavelength.

Many studies have noticed that the lensing effect can greatly enhance the absorption of BC. However, there is also an opposite effect, which is commonly neglected. As shown in of Fig. 3(d), as  $k_{BrC}$  increases, the value of  $E_{abs\_lensing}$  can be below 1. This indicates that the absorption of BC internally mixed with BrC coatings may be less than the sum of the absorption of BrC coatings and BC when  $k_{BrC}$  is large. This phenomenon can be explained from physical insights. When the absorption of the coatings is weak, the light can penetrate the coatings into the BC materials, and the absorption of BC is significantly enhanced by the lensing effect. However, as the coating absorption increases, the light is blocked by the outer coatings. Therefore, the light can not fully and deeply penetrate the absorbing coatings on BC. As a result, the total absorption is less than the sum of the absorption of coatings and BC that are calculated separately. Therefore, there is a need to classify the lensing effect into a convex lensing effect and sunglasses effect, which represents the absorption enhancements and blocking effects of coatings, respectively.

Although core-shell sphere model has been debated for a long time, it is still widely used in climate models. By Combining the electron tomography (ET) and discrete dipole approximation (DDA) method, Adachi et al. (2010) found that the absorption of BC with fluffy structures is significantly enhanced by a core-shell structure at  $\lambda = 0.55 \mu m$ . However, for aged BC with thick coatings, BC absorption is underestimated at the UV, visible, and IR wavelengths (Kahnert et al., 2012). Nevertheless, the effects of coating absorption on the applicability of the core-shell sphere model have not been evaluated. As shown in Fig. 4,  $C_{abs}$  for thinly-coated BC is enhanced by a core-shell sphere structure in the visible spectral region, which agrees with the study



of Adachi et al. (2010), while it is underestimated in the ultraviolet region. In addition, the ratio of  $C_{abs}$  of thinly-coated BC to core-shell sphere model increases with  $k_{BrC}$ . However, the applicability of the core-shell sphere model to thickly-coated BC is diverse. Consistent with Kahnert et al. (2012), thickly-coated BC absorption is underestimated by core-shell sphere model when coated with non-absorbing materials. Nevertheless, as  $k_{BrC}$  increases, the underestimation becomes insignificant. The reason may be that less light can penetrate deeply into the BC as the  $k_{BrC}$  increases, which leads to less variation in absorption. Therefore, the morphological effects of BC are relatively small.

The  $E_{abs}$ , compared with that for core-shell sphere model, is also calculated. For thinly-coated BC, the  $E_{abs}$  is significantly overestimated by core-shell sphere model. However, this overestimation is alleviated by an increasing  $k_{BrC}$ . For BC that is thickly-coated with non-absorbing materials, the  $E_{abs}$  is underestimated by core-shell sphere model at all wavelengths, while it decreases as  $k_{BrC}$  becomes larger. The  $E_{abs}$  can be overestimated by core-shell sphere model in the ultraviolet spectral region when  $k_{BrC}$  is large. Therefore, the absorption characteristics of BC are significantly affected by the absorption of coatings. To agree with the measurements, typical  $k_{BrC}$  values are assumed according to Kirchstetter et al. (2004), as shown in Fig. 5. In this work,  $k_{BrC}$  values of 0.168, 0.114, 0.0354 and 0.001 were assumed for 4 typical wavelengths ( $\lambda = 350 \text{ nm}$ ,  $404 \text{ nm}$ ,  $532 \text{ nm}$  and  $700 \text{ nm}$ , respectively) via interpolation.

### 3.2 Bulk radiative properties

The sensitivity study conducted by Zhang et al. (2017) showed that the  $E_{abs}$  for aged BC was significantly affected by the size distribution. They reported different  $E_{abs}$  values of  $\sim 1.7 - 2.4$  and  $\sim 2.0 - 2.7$  for accumulated and coarse modes, respectively. By setting the fractal dimension to be 2.2 and  $f_{BC}$  to be 40%, the variations in BC absorption enhancements for different particle size distributions are shown in Fig. 6. Generally, increased absorption enhancement can be observed at shorter wavelengths, which is in agreement with the study of You et al. (2016). By defining the monomers radii, Kahnert (2010a) demonstrated that the absorption cross-section is significantly affected by the particle size, and the cubic fit can greatly describe the relations among equivalent volume radii for freshly emitted BC. However, for the absorption enhancement of thinly-coated BC, the effects of size distribution are not obvious. With variations in  $r_g$  and  $\sigma_g$ , the absorption enhancement changes at ranges of  $\sim 1.563 - 1.603$ ,  $\sim 1.427 - 1.465$ ,  $\sim 1.2440 - 1.275$  and  $\sim 1.146 - 1.169$  for  $\lambda = 0.35 \text{ }\mu\text{m}$ ,  $0.404 \text{ }\mu\text{m}$ ,  $0.532 \text{ }\mu\text{m}$  and  $0.7 \text{ }\mu\text{m}$ , respectively. The relative errors in the absorption enhancements caused by the size distribution are 2.56%, 2.66%, 2.81% and 2.01%, respectively. The effects of the size distribution on the absorption enhancement of thinly-coated BC are similar at different wavelengths. Generally,  $E_{abs}$  has the largest value when both  $r_g$  and  $\sigma_g$  are extremely small or extremely large.

The absorption of BrC and BC are considered separately in most cases. To investigate the difference between the absorption of internally mixed BC and the total absorption of BrC and BC (calculated separately),  $E_{abs\_lensing}$  is also calculated.  $E_{abs\_lensing}$  shares a similar dependence on size distribution as  $E_{abs}$  does for visible wavelengths. The reason is that the  $E_{abs}$  mainly derives from lensing effects due to the weak absorption of coatings. However, for ultraviolet wavelengths, there is a completely different pattern. The largest  $E_{abs\_lensing}$  occurs when both  $r_g$  and  $\sigma_g$  are extremely small. Given the understanding of the values, the effects of size distribution are also not obvious.  $E_{abs\_lensing}$  changes in the ranges of  $\sim 1.080 - 1.146$ ,  $\sim 1.107 - 1.148$ ,  $\sim 1.145 - 1.164$  and  $\sim 1.144 - 1.1652$  for  $\lambda = 0.35 \text{ }\mu\text{m}$ ,  $0.404 \text{ }\mu\text{m}$ ,  $0.532 \text{ }\mu\text{m}$  and  $0.7 \text{ }\mu\text{m}$ , respectively.





The relative errors of the different size distributions are less than 6.11%, 3.70%, 1.66% and 1.89%, respectively. In addition, for thinly-coated BC,  $E_{abs\_lensing}$  is greater than 1, and the values are in the range of  $\sim 1.08 - 1.166$ . This indicates that the blocking effects of BrC coatings are weaker than the strengthening effects caused by lensing effects, as the coatings are thin.

Figure 7 illustrates the effects of size distribution for thickly-coated BC. Compared with thinly-coated BC, there is a different effect pattern for thickly-coated BC. For ultraviolet wavelengths (e.g.,  $\lambda = 0.35 \text{ } \mu\text{m}$  and  $0.404 \text{ } \mu\text{m}$ ), absorption enhancements decrease as  $r_g$  or  $\sigma_g$  increases. This indicates that as the particle becomes larger or the size distribution becomes wider, the absorption enhancements become weaker. However, for the visible wavelengths, the effects of the size distribution is quite complicated. The absorption enhancements are relatively small when both  $r_g$  and  $\sigma_g$  are extremely large or small. The peak value commonly occurs when  $\sigma_g$  is extremely small. Zhang et al. (2017) concluded that the  $E_{abs}$  of aged BC is more sensitive to the size distribution in the accumulation mode (where the  $\sigma_g$  is relatively small), while the  $E_{abs}$  of coarsely coated BC aggregates (i.e., with large  $\sigma_g$ ) show little variation with  $r_g$ . This is precisely true for BC with weak absorbing coatings, as shown in the results for  $\lambda = 0.7 \text{ } \mu\text{m}$ . However, for BC with absorbing coatings,  $E_{abs}$  is sensitive to the size distribution for both modes. When fixing the  $f_{BC}$  to be 6% ( $D_p/D_c = 2.5544$ ), as  $r_g$  and  $\sigma_g$  vary, the absorption enhancements change in the ranges of  $\sim 3.7 - 7.1$ ,  $\sim 3.85 - 5.80$ ,  $\sim 3.06 - 3.74$  and  $\sim 1.63 - 2.59$  for  $\lambda = 0.35 \text{ } \mu\text{m}$ ,  $0.404 \text{ } \mu\text{m}$ ,  $0.532 \text{ } \mu\text{m}$  and  $0.7 \text{ } \mu\text{m}$ , respectively, and the uncertainties in  $E_{abs}$  can reach up to 91.9%, 50.7%, 22.2% and 60.7%, respectively. The calculated results are greater than the measured absorption enhancements of  $\sim 1.05 - 3.5$  in the visible region (Khalizov et al., 2009; Xue et al., 2009; Bond et al., 2013). Our calculations indicate that the absorption enhancements can reach approximately 3.7 for  $\lambda = 0.532 \text{ } \mu\text{m}$ . The reason is mainly due to three aspects: (1) all coatings were assumed to be BrC coatings in this work, and the absorption of coatings was obvious in the ultraviolet band and near the ultraviolet spectral regions. However, in the atmosphere, the coatings are not only BrC coatings but also inorganic material coatings (e.g., sulfates), which present weak absorption in the ultraviolet to near-infrared regions (Aouizerats et al., 2010). (2) The results in Fig. 7 are obtained by assuming that all the BC are thickly coated, while in the atmosphere, not all BC are thickly-coated. According to China et al. (2013), approximately 50% of freshly emitted BC particles are thickly-coated. In many cases, BC is thinly-coated. Therefore, the absorption enhancement in this work is relatively higher than that of the measurements. (3) For the sensitivity analysis, the size distributions cover a broaden range in this work, while the real size distributions in the atmosphere are in a narrower range; therefore, the range of  $E_{abs}$  observed in the atmosphere is relatively narrow. Even though the calculated results do not completely reflect the real absorption enhancements, based on the sensitivity analysis, they can give the upper values of the absorption enhancements and improve the understanding on the effects of BrC coatings. In addition, they can provide theoretical explanations for the high absorption enhancements. For example, the measured absorption enhancements can reach approximately 3.5, while the calculated results based on non-absorbing coatings are commonly less than 3.0. To better correspond to the measurements, we discussed the influences of mixing states for a typical size distribution in the next section (see Fig. 10 and Fig. 12).

The  $E_{abs\_lensing}$  value for thickly-coated BC has the similar dependences on the size distribution compared to  $E_{abs}$ .  $E_{abs\_lensing}$  changes substantially as  $r_g$  or  $\sigma_g$  varies. As  $r_g$  or  $\sigma_g$  decreases,  $E_{abs\_lensing}$  increases from 0.45 to 1.37 and from 0.51 to 1.61 for  $\lambda = 0.35 \text{ } \mu\text{m}$  and  $0.404 \text{ } \mu\text{m}$  respectively. For visible wavelengths, the effects of size distribution are rather complicated. As  $r_g$  and  $\sigma_g$  vary,  $E_{abs\_lensing}$  can change from 1.455 to 2.025 and from 1.63 to 2.52 for  $\lambda = 0.532 \text{ } \mu\text{m}$



and 0.7  $\mu\text{m}$ , respectively. Variation in the size distribution can lead to  $E_{abs\_lensing}$  differences of 204.4%, 215.7%, 39.2% and 56.4% for  $\lambda = 0.35 \mu\text{m}$ , 0.404  $\mu\text{m}$ , 0.532  $\mu\text{m}$  and 0.7  $\mu\text{m}$ , respectively. In addition, for the ultraviolet wavelengths,  $E_{abs\_lensing}$  can be less than 1. This phenomenon is caused by the large absorption of coatings, which blocks the light penetrating deeply in to the inner materials. As a result, the total absorption is less than the sum of the absorption of coatings and BC.

5 In climate models, the  $\sigma_g$  is commonly assumed to be a fixed value, and the BC size distribution is commonly assumed to be in accumulation mode (Liu et al., 2012). To further understand of the effects of size distribution, we fixed  $\sigma_g$  to be 1.5, and the variations in  $E_{abs}$  and  $E_{abs\_lensing}$  with different  $f_{BC}$  values at various  $r_g$  are shown in Figs. 8-9. For thinly-coated BC,  $E_{abs}$  seems to be insensitive to  $r_g$ . As  $r_g$  changes, the variations of  $E_{abs}$  are below 2% for different  $f_{BC}$  and  $\lambda$ . However, the effects of  $r_g$  cannot be neglected for thickly-coated BC. Assuming  $f_{BC}$  is 0.06, as  $r_g$  decreases from 0.1 to 0.03,  $E_{abs}$   
10 increases from 4.25 to 7.11 and from 4.44 to 6.28 for  $\lambda = 0.35 \mu\text{m}$  and  $\lambda = 0.404 \mu\text{m}$ , respectively, which leads to approximate 1.673 and 1.414 times increments, respectively. The effects of  $r_g$  are relatively small for visible wavelengths. However, it can still introduce a relative difference of approximately 23% for  $\lambda = 0.7 \mu\text{m}$  as  $r_g$  varies. In addition, contrary to thickly-coated BC with absorbing coatings,  $E_{abs}$  increases with  $r_g$  for BC with non-absorbing coatings, which is consistent with the results reported by Zhang et al. (2017).

15  $E_{abs\_lensing}$  is in the range of  $\sim 1.03 - 1.27$  for thinly-coated BC. Generally, the effects of  $r_g$  are more sensitive at ultraviolet wavelengths and for BC with thicker coatings. By fixing  $f_{BC}$  to be 20%, as  $r_g$  increases from 0.03 to 0.1,  $E_{abs\_lensing}$  decreases from 1.18 to 1.1 when  $\lambda = 0.35 \mu\text{m}$ , which results in an approximate 7.3% variation. However, the relative deviations are within 2% for  $\lambda = 0.532 \mu\text{m}$  and 0.7  $\mu\text{m}$ . Nevertheless, the effects of  $r_g$  are rather obvious for thickly-coated BC. The effects of  $r_g$  are related to wavelength.  $E_{abs\_lensing}$  decreases with  $r_g$  at ultraviolet wavelengths, while it increases as the particles become  
20 large for visible wavelengths. Based on physical insights, the reason may be due to two aspects. When the wavelength is at ultraviolet region, the absorption of the coatings is large, therefore, the blocking effects of the coatings is obvious. Given identical  $f_{BC}$  values, the superficial area of the outer coating becomes larger as  $r_g$  increases. As a result, the blocking effects of the outer coatings increases. Therefore, the  $E_{abs\_lensing}$  decreases. For visible wavelengths, the absorption of the coatings is negligible, and the light can penetrate deeply into BC. At that point, the main factor is the enhancement of the lensing effects,  
25 and the larger particles may cause a larger superficial area, which leads to enhanced  $E_{abs\_lensing}$ .

Figure 9 also demonstrates that there are different dependences on  $f_{BC}$  for different wavelengths. As the coatings become thicker (i.e.,  $f_{BC}$  decreases),  $E_{abs\_lensing}$  becomes weaker for  $\lambda = 0.35 \mu\text{m}$  and 0.404  $\mu\text{m}$ , while when  $\lambda = 0.7 \mu\text{m}$ ,  $E_{abs\_lensing}$  is enhanced as  $f_{BC}$  decreases. This phenomenon can also be explained from physical insights. When the wavelength is short, increased thickness of the coatings may lead to a greater blocking effect, which weakens the total absorption of the coatings and BC. However, for visible wavelengths, enhanced  $E_{abs\_lensing}$  can be obtained by increasing the coatings due  
30 to the negligible blocking effects of the coatings. In addition,  $E_{abs\_lensing}$  increases with wavelength due to the decrease in coating absorption (see Fig. 3). When setting  $\sigma_g$  to be 1.5, for different  $r_g$ ,  $E_{abs\_lensing}$  is in the ranges of  $\sim 0.42 - 1.1$ ,  $\sim 0.45 - 1.35$ ,  $\sim 1.41 - 1.95$  and  $\sim 1.75 - 2.5$  for  $\lambda = 0.35 \mu\text{m}$ , 0.404  $\mu\text{m}$ , 0.532  $\mu\text{m}$  and 0.7  $\mu\text{m}$ , respectively. For ultraviolet wavelengths, the  $E_{abs\_lensing}$  can be less than 1. This indicates that the blocking effects of absorbing coatings may be greater than  
35 the enhancements of the lensing effects. Therefore, when BC coated with BrC, we should not only focus on the enhancements



of the lensing effects but also carefully consider the blocking effects of the coatings. In addition, for both thinly-coated and thickly-coated BC,  $E_{abs\_lensing}$  is quite sensitive to the composition ratio of the coatings.

Figure 10 compares the  $E_{abs}$  and  $E_{abs\_lensing}$  for thinly-coated BC with different fractal dimensions at different composition ratios.  $D_p/D_c$  represents the shell-core ratio (i.e., the equivalent particle diameter divided by equivalent BC diameter). Following Liu et al. (2018), an  $r_g$  of  $0.06\ \mu\text{m}$  and an  $\sigma$  of 1.5 are assumed to reflect the real size distribution of BC. It is expected that as the coatings increase,  $E_{abs}$  becomes much stronger. With  $D_p/D_c$  varying from 1.0 to 1.71,  $E_{abs}$  variations of  $\sim 1 - 2.5$ ,  $\sim 1 - 2.2$ ,  $\sim 1 - 1.6$  and  $\sim 1 - 1.285$  are obtained for  $\lambda = 0.35\ \mu\text{m}$ ,  $0.404\ \mu\text{m}$ ,  $0.532\ \mu\text{m}$  and  $0.7\ \mu\text{m}$ , respectively. The  $E_{abs}$  for thinly-coated BC with weakly-absorbing materials (i.e.,  $\lambda = 0.7\ \mu\text{m}$ ) is significantly lower than that for core-shell sphere, as reported by Zhang et al. (2017), where  $E_{abs}$  can reach approximately 1.5 when  $D_p/D_c = 1.6$  at  $\lambda = 0.55\ \mu\text{m}$ . Even though the results are gained at two different wavelengths, the  $E_{abs}$  for BC that is coated with weakly absorption coatings should not diverge substantially between  $\lambda = 0.55\ \mu\text{m}$  and  $\lambda = 0.7\ \mu\text{m}$  (see Fig. 13). Therefore, the differences from the previous study are mainly caused by the BC shape, as demonstrated in Fig. 4. When the relative contents of BC vary, substantial variations in  $E_{abs\_lensing}$  can also be observed. As  $D_p/D_c$  varies from 1.0 to 1.71,  $E_{abs\_lensing}$  increases from 1 to 1.13, 1 to 1.18, 1 to 1.27 and 1 to 1.285 for  $\lambda = 0.35\ \mu\text{m}$ ,  $0.404\ \mu\text{m}$ ,  $0.532\ \mu\text{m}$  and  $0.7\ \mu\text{m}$ , respectively, and enhancements of approximately 13%, 18%, 27% and 28.5% can be obtained. For different wavelengths, the effects of  $D_f$  may vary.  $E_{abs\_lensing}$  increases with  $D_f$  at visible wavelengths, as the more compact structure can lead to a greater lensing interaction. For ultraviolet wavelengths, as the structure becomes more compact, the interaction of absorbing coatings also increases; therefore, the blocking effects of outer coatings are greater. Therefore, the  $E_{abs\_lensing}$  can decrease with  $D_f$  when  $D_f$  is greater than a value.

Even though Cheng et al. (2014) and Luo et al. (2018b) showed that the effects of  $D_f$  on  $C_{abs}$  are not obvious for thinly-coated BC, for  $E_{abs}$  of thinly-coated BC, the sensitivity of  $D_f$  has not been investigated. To quantify the effects of  $D_f$ , the relative deviations between  $D_f = 1.8$  and  $D_f = 2.6$  are also calculated for thinly-coated BC. From Fig. 10, we found that the differences in  $E_{abs}$  and  $E_{abs\_lensing}$  among different values of  $D_f$  are larger for thicker coatings. Therefore, to evaluate the maximum error, the  $f_{BC}$  is fixed to be 20%. As shown in Fig. 11, except for  $\lambda = 0.35\ \mu\text{m}$ , the differences in  $E_{abs}$  and  $E_{abs\_lensing}$  between  $D_f = 1.8$  and  $D_f = 2.6$  are all below 5%. These errors are much less than that for thickly-coated BC, where the difference can reach approximately 20% for coarse mode BC (Zhang et al., 2017). In addition, the difference between  $D_f = 1.8$  and  $D_f = 2.6$  seems to be larger for large particles. Although the differences in  $E_{abs\_lensing}$  can reach approximately 9% for  $\lambda = 0.35\ \mu\text{m}$ , when  $r_g$  is below  $0.07\ \mu\text{m}$ , the relative deviation between  $D_f = 1.8$  and  $D_f = 2.6$  is within 5%. As a result,  $E_{abs}$  and  $E_{abs\_lensing}$  do not change substantially with  $D_f$  when  $r_g$  is in the range of  $0.05 \sim 0.06\ \mu\text{m}$ , which is widely accepted for bare BC (Alexander et al., 2008; Coz and Leck, 2011).

Figure 12 demonstrates the absorption enhancements of thickly-coated BC at different wavelengths for different composition ratios. Similar to thinly-coated BC,  $E_{abs}$  increases with increasing  $D_p/D_c$  or decreasing  $\lambda$ . When setting  $r_g = 0.06\ \mu\text{m}$  and  $\sigma_g = 1.5$ , as  $D_p/D_c$  varies from 2.15 to 2.71,  $E_{abs}$  increases from 3.4 to 5.4 and 3.25 to 5.2 for  $\lambda = 0.35\ \mu\text{m}$  and  $\lambda = 0.404\ \mu\text{m}$ , respectively, which results in an approximate 1.6 times  $E_{abs}$  enhancements, while  $E_{abs}$  varies from 2.78 to 3.96 and 2.2 to 2.4 for  $\lambda = 0.532\ \mu\text{m}$  and  $0.7\ \mu\text{m}$ , respectively. In addition, the  $E_{abs}$  seems to be more sensitive to the composition ratios at ultraviolet wavelengths. This may be caused by the absorption of coatings, which can substantially enhance the total



absorption. In addition, combined of  $E_{abs}$  values of thinly-coated and thickly-coated BC,  $E_{abs}$  range for BC with BrC coatings is much wider than that for BC with non-absorbing coatings ( $E_{abs}$  of  $\sim 1 - 2.4$ ) (Zhang et al., 2017, 2018)

There is a different dependence on  $D_p/D_c$  for  $E_{abs\_lensing}$ .  $E_{abs\_lensing}$  increases with  $D_p/D_c$  at visible wavelengths, while decreases as the coatings become thicker at ultraviolet wavelengths. For visible wavelengths, the  $E_{abs\_lensing}$  is greater than 1 due to the small blocking effects of BrC. By setting  $r_g$  to be  $0.06 \mu m$  and  $\sigma_g$  to be 1.5,  $E_{abs\_lensing}$  ranges from  $\sim 1.75 - 1.9$  and  $\sim 2.05 - 2.4$  for  $\lambda = 0.532 \mu m$  and  $0.7 \mu m$ , respectively. This indicates that the total absorption of BC and BrC can be substantially enhanced by the lensing effects. However, for ultraviolet wavelengths, the  $E_{abs\_lensing}$  is less than 1.  $E_{abs\_lensing}$  is within  $\sim 0.65 - 0.76$  and  $\sim 0.88 - 1.02$  for  $\lambda = 0.35 \mu m$  and  $\lambda = 0.404 \mu m$ , respectively. This demonstrates the absorbing coatings can significantly block the light into BC. Therefore, the total absorption is less than the sum of BrC absorption and BC absorption. In recent studies, the enhancements of lensing effects has gained increasing attention. However, few studies have investigated the blocking effects of absorbing coatings. As a matter of fact, the blocking effect of absorbing coatings is also a significant factor that affects the total absorption, as the  $E_{abs\_lensing}$  can be below 0.5 (see Fig. 7), which indicates that the absorption of BC can be reduced by 0.5 times. As a result, the blocking effect of absorbing coatings should also be taken into consideration in climate studies.

You et al. (2016) demonstrated there are different wavelength dependencies for BC that is coated with absorbing and weak absorbing materials.  $E_{abs}$  for BC coated with humic acid was observed to vary from 3.0 to approximately 1.6 as  $\lambda$  increased from  $0.554 \mu m$  to  $0.84 \mu m$ , while it seemed to be essentially wavelength-independent for BC that is coated with sodium chloride. Figure 13 compares the wavelength dependencies of BC coated with non-absorbing materials and BrC. For thinly-coated BC, there are substantial wavelength dependencies for BC coated with BrC. By setting  $f_{BC}$  to be 40%,  $E_{abs}$  increases from 1.15 to 1.57 with  $\lambda$  varying from  $0.7 \mu m$  to  $0.35 \mu m$ , which results in approximately 49.6% increase. However, when coated with non-absorbing materials,  $E_{abs}$  exhibits small wavelength-dependences. This leads to approximate 8.7% increases as  $\lambda$  decreases from  $0.7 \mu m$  to  $0.35 \mu m$ . Furthermore, for thickly-coated BC,  $E_{abs}$  is significantly wavelength-dependent for BC with BrC coatings. The decrease in  $\lambda$  from  $0.7 \mu m$  to  $0.35 \mu m$  would result in approximate 100% increase in  $E_{abs}$ , while  $E_{abs}$  seems to be essentially wavelength-independent for BC with non-absorbing coatings; it is approximately 2.4 when  $f_{BC} = 6\%$ , which is consistent with the value reported by Zhang et al. (2017). Therefore, the variation in  $k_{BrC}$  should be mainly responsible for the significant wavelength dependencies of  $E_{abs}$  for BC with BrC coatings when the wavelength is long. For ultraviolet wavelengths ( $\lambda$  from  $0.35 \mu m$  to  $0.404 \mu m$ ), wavelength dependence of  $E_{abs}$  is relatively small, as the  $E_{abs}$  may increase with wavelength when  $k_{BrC}$  is fixed at a large value (see Fig. 3), which can reduce the wavelength dependence. Therefore, the contribution of  $k_{BrC}$  to the wavelength dependence should be further analyzed at ultraviolet wavelengths in the future. In addition, the  $E_{abs\_lensing}$  of BC coated with BrC is also wavelength-dependent. There is an approximately 7.5% increase in  $E_{abs\_lensing}$  as  $\lambda$  increases from  $0.35 \mu m$  to  $0.7 \mu m$ . For thickly-coated BC,  $E_{abs\_lensing}$  is more significantly affected by wavelength, and varies from approximately 0.6 to approximately 2.4 when  $f_{soot} = 6\%$ .



#### 4 Summary and Discussion

Using MSTM method, the  $E_{abs}$  and  $E_{abs\_lensing}$  of BC with BrC coatings were investigated at  $\lambda = 0.35\mu m, 0.404\mu m, 0.532\mu m$  and  $0.7\mu m$ , respectively. The main findings of this work are as follows:

1. Generally,  $E_{abs}$  increases with  $k_{BrC}$  while  $E_{abs\_lensing}$  decreases as  $k_{BrC}$  becomes larger. For the thinly-coated BC,  $E_{abs\_lensing}$  is greater than 1 due to the enhancements of the lensing effects. However, for thickly-coated BC, the  $E_{abs\_lensing}$  can be less than 1. It indicates the total absorption of BrC and BC is less than sum of BrC and BC absorption individually, which is opposite to BC that is coated with weakly-absorbing coatings. This phenomenon may be caused by the blocking effects of outer coatings. As the absorption of coatings increases, less light can penetrate into BC materials. Therefore, the total absorption of BrC and BC is weakened, resulting in  $E_{abs\_lensing}$  of less than 1. This effect is named "sunglasses effect" in this study.
2.  $C_{abs}$  of thinly-coated BC is underestimated by core-shell sphere model in the ultraviolet region while overestimated in the visible region. In addition, the ratio of  $C_{abs}$  of thinly-coated BC to that of core-shell sphere model increases with  $k_{BrC}$ .  $E_{abs}$  of thinly-coated BC is enhanced by core-shell sphere while the enhancements are alleviated by increasing  $k_{BrC}$ . There are different dependencies for thickly-coated BC.  $C_{abs}$  of thickly-coated BC is underestimated by core-shell sphere model for all wavelengths while the underestimation becomes negligible as  $k_{BrC}$  turns very large.  $E_{abs}$  of thickly-coated BC with non-absorbing materials is underestimated by core-shell assumption. However, the ratio of  $E_{abs}$  of thickly-coated BC to core-shell sphere model decreases with increasing  $k_{BrC}$ , and  $E_{abs}$  is enhanced by core-shell sphere in the visible region, when the absorption of coatings is large.
3. To make our calculation more consistent with real circumstance, the bulk absorption was calculated and the  $k_{BrC}$  is selected by interpolation based on the study of Kirchstetter et al. (2004). For thinly-coated BC, the effects of size distribution on  $E_{abs}$  are not obvious. The uncertainties of size distribution result in  $E_{abs}$  differences of less than 2.56%, 2.52%, 2.32% and 2.16% for  $\lambda = 0.35\mu m, 0.404\mu m, 0.532\mu m$  and  $0.7\mu m$ , respectively. However,  $E_{abs}$  of thickly-coated BC is quite sensitive to the size distribution.  $E_{abs}$  differences of approximately 92% can be obtained as  $r_g$  and  $\sigma_g$  vary for  $\lambda = 0.35\mu m$ . In addition, different from  $E_{abs}$  of 2.2 ~ 2.4 for thickly-coated BC with weak absorbing coatings,  $E_{abs}$  of 3.4 ~ 5.4 is observed for BC with BrC coatings at  $\lambda = 0.35\mu m$ . For thinly coated BC,  $E_{abs}$  of BC with weak absorbing coatings is in the range of approximately ~1 - 1.3 for  $\lambda = 0.7\mu m$  (i.e. BC with weakly-absorbing coatings) while a wider range of ~1 - 2.5 is obtained for  $\lambda = 0.35\mu m$ . In summary,  $E_{abs}$  range of BC with BrC coatings is much wider than that of BC with non-absorbing coatings.
4.  $E_{abs}$  of BC with BrC coatings is more wavelength-dependent than those with non-absorbing coatings. For thinly coated BC,  $E_{abs}$  of BC with non-absorbing coatings leads to approximately 8.7% increase as  $\lambda$  decreases from  $0.7\mu m$  to  $0.35\mu m$  while the difference can reach approximately 50% for BC with BrC coatings. For thickly coated BC, the decrease of  $\lambda$  from  $0.7\mu m$  to  $0.35\mu m$  would result in approximately 100% increase of  $E_{abs}$  for BC with BrC coatings. However,  $E_{abs}$  of BC with non-absorbing coatings seems to be essentially wavelength-independent. In addition, for thinly



coated BC, the effects of  $D_f$  are not obvious for  $E_{abs}$  and  $E_{abs\_lensing}$ . The uncertainties of  $D_f$  lead to  $E_{abs}$  and  $E_{abs\_lensing}$  differences of less than 7.4% and 9%, respectively.

## 5 Acknowledgments

This work was financially supported by the National Key Research and Development Plan (Grant No. 2016YFC0800100 and 2017YFC0805100); National Natural Science Foundation of China (Grant No. 41675024 and U1733126); Fundamental Research Funds for the Central Universities (Grant No. WK2320000035). We particularly thank Dr. D. W. Mackowski and Dr. M. I. Mishchenko for the MSTM code. We also acknowledge the support of supercomputing center of USTC.





## References

- Adachi, K. and Buseck, P. R.: Internally mixed soot, sulfates, and organic matter in aerosol particles from Mexico City, *Atmospheric Chemistry and Physics*, 8, 6469–6481, <GotoISI>://WOS:000260927800011, 2008.
- Adachi, K., Chung, S. H., and Buseck, P. R.: Shapes of soot aerosol particles and implications for their effects on climate, *Journal of Geophysical Research: Atmospheres*, 115, 2010.
- Alexander, D. T. L., Crozier, P. A., and Anderson, J. R.: Brown carbon spheres in East Asian outflow and their optical properties, *Science*, 321, 833–836, <GotoISI>://WOS:000258261000045, 2008.
- Andreae, M. O. and Gelencser, A.: Black carbon or brown carbon? The nature of light-absorbing carbonaceous aerosols, *Atmospheric Chemistry and Physics*, 6, 3131–3148, <GotoISI>://WOS:000239346600001, 2006.
- 10 Aouizerats, B., Thouron, O., Tulet, P., Mallet, M., Gomes, L., and Henzing, J. S.: Development of an online radiative module for the computation of aerosol optical properties in 3-D atmospheric models: validation during the EUCAARI campaign, *Geoscientific Model Development*, 3, 553–564, <GotoISI>://WOS:000285965100012, 2010.
- Bi, L. and Yang, P.: Tunneling effects in electromagnetic wave scattering by nonspherical particles: A comparison of the Debye series and physical-geometric optics approximations, *Journal of Quantitative Spectroscopy and Radiative Transfer*, 178, 93–107, <GotoISI>://WOS:000376705900009, 2016.
- 15 Bond, T. C. and Bergstrom, R. W.: Light absorption by carbonaceous particles: An investigative review, *Aerosol Science and Technology*, 40, 27–67, <GotoISI>://WOS:000233906000001, 2006.
- Bond, T. C., Covert, D. S., Kramlich, J. C., Larson, T. V., and Charlson, R. J.: Primary particle emissions from residential coal burning: Optical properties and size distributions, *Journal of Geophysical Research-Atmospheres*, 107, <GotoISI>://WOS:000180485800015, 2002.
- 20 Bond, T. C., Habib, G., and Bergstrom, R. W.: Limitations in the enhancement of visible light absorption due to mixing state, *Journal of Geophysical Research-Atmospheres*, 111, <GotoISI>://WOS:000241866200010, 2006.
- Bond, T. C., Doherty, S. J., Fahey, D. W., Forster, P. M., Bernsten, T., DeAngelo, B. J., Flanner, M. G., Ghan, S., Karcher, B., Koch, D., Kinne, S., Kondo, Y., Quinn, P. K., Sarofim, M. C., Schultz, M. G., Schulz, M., Venkataraman, C., Zhang, H., Zhang, S., Bellouin, N., Guttikunda, S. K., Hopke, P. K., Jacobson, M. Z., Kaiser, J. W., Klimont, Z., Lohmann, U., Schwarz, J. P., Shindell, D., Storelvmo, T., Warren, S. G., and Zender, C. S.: Bounding the role of black carbon in the climate system: A scientific assessment, *Journal of Geophysical Research-Atmospheres*, 118, 5380–5552, <GotoISI>://WOS:000325212600025, 2013.
- 25 Cappa, C. D., Onasch, T. B., Massoli, P., Worsnop, D. R., Bates, T. S., Cross, E. S., Davidovits, P., Hakala, J., Hayden, K. L., Jobson, B. T., Kolesar, K. R., Lack, D. A., Lerner, B. M., Li, S. M., Mellon, D., Nuaaman, I., Olfert, J. S., Petaja, T., Quinn, P. K., Song, C., Subramanian, R., Williams, E. J., and Zaveri, R. A.: Radiative Absorption Enhancements Due to the Mixing State of Atmospheric Black Carbon, *Science*, 337, 1078–1081, <GotoISI>://WOS:000308125800042, 2012.
- 30 Chakrabarty, R. K., Moosmuller, H., Garro, M. A., Arnott, W. P., Walker, J., Susott, R. A., Babbitt, R. E., Wold, C. E., Lincoln, E. N., and Hao, W. M.: Emissions from the laboratory combustion of wildland fuels: Particle morphology and size, *Journal of Geophysical Research-Atmospheres*, 111, <GotoISI>://WOS:000236880400003, 2006.
- Chen, B., Bai, Z., Cui, X. J., Chen, J. M., Andersson, A., and Gustafsson, O.: Light absorption enhancement of black carbon from urban haze in Northern China winter, *Environmental Pollution*, 221, 418–426, <GotoISI>://WOS:000392767900044, 2017.
- Cheng, T. H., Wu, Y., and Chen, H.: Effects of morphology on the radiative properties of internally mixed light absorbing carbon aerosols with different aging status, *Optics Express*, 22, 15 904–15 917, <GotoISI>://WOS:000338055900072, 2014.



- Cheng, T. H., Wu, Y., Gu, X. F., and Chen, H.: Effects of mixing states on the multiple-scattering properties of soot aerosols, *Optics Express*, 23, 10 808–10 821, <GotoISI>://WOS:000353299300126, 2015.
- Cheng, Y., He, K. B., Engling, G., Weber, R., Liu, J. M., Du, Z. Y., and Dong, S. P.: Brown and black carbon in Beijing aerosol: Implications for the effects of brown coating on light absorption by black carbon, *Science of the Total Environment*, 599, 1047–1055, <GotoISI>://WOS:000405253500001, 2017.
- China, S., Mazzoleni, C., Gorkowski, K., Aiken, A. C., and Dubey, M. K.: Morphology and mixing state of individual freshly emitted wildfire carbonaceous particles, *Nature Communications*, 4, <GotoISI>://WOS:000323715900002, 2013.
- China, S., Salvadori, N., and Mazzoleni, C.: Effect of Traffic and Driving Characteristics on Morphology of Atmospheric Soot Particles at Freeway On-Ramps, *Environmental Science and Technology*, 48, 3128–3135, <GotoISI>://WOS:000333776000007, 2014.
- 10 Chung, C. E., Ramanathan, V., and Decremier, D.: Observationally constrained estimates of carbonaceous aerosol radiative forcing, *Proceedings of the National Academy of Sciences of the United States of America*, 109, 11 624–11 629, <GotoISI>://WOS:000306837100034, 2012.
- Coz, E. and Leck, C.: Morphology and state of mixture of atmospheric soot aggregates during the winter season over Southern Asia—a quantitative approach, *Tellus Series B-Chemical and Physical Meteorology*, 63, 107–116, <GotoISI>://WOS:000286001900009, 2011.
- 15 Cui, X. J., Wang, X. F., Yang, L. X., Chen, B., Chen, J. M., Andersson, A., and Gustafsson, O.: Radiative absorption enhancement from coatings on black carbon aerosols, *Science of the Total Environment*, 551, 51–56, <GotoISI>://WOS:000372589800007, 2016.
- Draine, B. T. and Flatau, P. J.: Discrete-Dipole Approximation for Scattering Calculations, *Journal of the Optical Society of America a-Optics Image Science and Vision*, 11, 1491–1499, <GotoISI>://WOS:A1994NE24300032, 1994.
- Forster, P., Ramaswamy, V., Artaxo, P., Berntsen, T., Betts, R., Fahey, D. W., Haywood, J., Lean, J., Lowe, D. C., Myhre, G., et al.: Changes in atmospheric constituents and in radiative forcing. Chapter 2, in: *Climate Change 2007. The Physical Science Basis*, 2007.
- 20 Fuller, K. A., Malm, W. C., and Kreidenweis, S. M.: Effects of mixing on extinction by carbonaceous particles, *Journal of Geophysical Research-Atmospheres*, 104, 15 941–15 954, <GotoISI>://WOS:000081535000004, 1999.
- He, C., Liou, K. N., Takano, Y., Zhang, R., Zamora, M. L., Yang, P., Li, Q., and Leung, L. R.: Variation of the radiative properties during black carbon aging: theoretical and experimental intercomparison, *Atmospheric Chemistry and Physics*, 15, 11 967–11 980, <GotoISI>://WOS:000364316800029, 2015.
- 25 Hentschel, H. G. E.: Fractal Dimension of Generalized Diffusion-Limited Aggregates, *Physical Review Letters*, 52, 212–215, <GotoISI>://WOS:A1984RY26700013, 1984.
- Jacobson, M. Z.: Strong radiative heating due to the mixing state of black carbon in atmospheric aerosols, *Nature*, 409, 695–697, <GotoISI>://WOS:000166816400037, 2001.
- 30 Jensen, M. H., Levermann, A., Mathiesen, J., and Procaccia, I.: Multifractal structure of the harmonic measure of diffusion-limited aggregates, *Physical Review E*, 65, <GotoISI>://WOS:000175146500028, 2002.
- Kahnert, M.: Modelling the optical and radiative properties of freshly emitted light absorbing carbon within an atmospheric chemical transport model, *Atmospheric Chemistry and Physics*, 10, 1403–1416, <GotoISI>://WOS:000274410000036, 2010a.
- Kahnert, M.: On the Discrepancy between Modeled and Measured Mass Absorption Cross Sections of Light Absorbing Carbon Aerosols, *Aerosol Science and Technology*, 44, 453–460, <GotoISI>://WOS:000277436300006, 2010b.
- 35 Kahnert, M.: Optical properties of black carbon aerosols encapsulated in a shell of sulfate: comparison of the closed cell model with a coated aggregate model, *Optics Express*, 25, 24 579–24 593, <GotoISI>://WOS:000412048500107, 2017.



- Kahnert, M., Nousiainen, T., Lindqvist, H., and Ebert, M.: Optical properties of light absorbing carbon aggregates mixed with sulfate: assessment of different model geometries for climate forcing calculations, *Optics Express*, 20, <GotoISI>://WOS:000303989300074, 2012.
- Khalizov, A. F., Xue, H. X., Wang, L., Zheng, J., and Zhang, R. Y.: Enhanced Light Absorption and Scattering by Carbon Soot Aerosol Internally Mixed with Sulfuric Acid, *Journal of Physical Chemistry A*, 113, 1066–1074, <GotoISI>://WOS:000263134900017, 2009.
- Kirchstetter, T. W., Novakov, T., and Hobbs, P. V.: Evidence that the spectral dependence of light absorption by aerosols is affected by organic carbon, *Journal of Geophysical Research-Atmospheres*, 109, <GotoISI>://WOS:000225190500010, 2004.
- Koylu, U. O., Faeth, G. M., Farias, T. L., and Carvalho, M. G.: Fractal and Projected Structure Properties of Soot Aggregates, *Combustion and Flame*, 100, 621–633, <GotoISI>://WOS:A1995QP52600009, 1995.
- 10 Krishnan, R. and Ramanathan, V.: Evidence of surface cooling from absorbing aerosols, *Geophysical Research Letters*, 29, <GotoISI>://WOS:000178888000023, 2002.
- Lack, D. A., Cappa, C. D., Cross, E. S., Massoli, P., Ahern, A. T., Davidovits, P., and Onasch, T. B.: Absorption Enhancement of Coated Absorbing Aerosols: Validation of the Photo-Acoustic Technique for Measuring the Enhancement, *Aerosol Science and Technology*, 43, 1006–1012, <GotoISI>://WOS:000269731800002, 2009.
- 15 Laczik, Z.: Discrete-dipole-approximation-based light-scattering calculations for particles with a real refractive index smaller than unity, *Applied Optics*, 35, 3736–3745, <GotoISI>://WOS:A1996UW46000056, 1996.
- Li, J., Liu, C., Yin, Y., and Kumar, K. R.: Numerical investigation on the Ångström Exponent of black carbon aerosol, *Journal of Geophysical Research-Atmospheres*, 121, 3506–3518, <GotoISI>://WOS:000375120200027, 2016.
- Liou, K. N., Takano, Y., and Yang, P.: Light absorption and scattering by aggregates: Application to black carbon and snow grains, *Journal of Quantitative Spectroscopy and Radiative Transfer*, 112, 1581–1594, <GotoISI>://WOS:000291714600009, 2011.
- 20 Liu, C., Chung, C. E., Yin, Y., and Schnaiter, M.: The absorption Ångström exponent of black carbon: from numerical aspects, *Atmospheric Chemistry and Physics*, 18, 6259–6273, <https://doi.org/10.5194/acp-18-6259-2018>, <https://www.atmos-chem-phys.net/18/6259/2018/>, 2018.
- Liu, D. T., Whitehead, J., Alfarra, M. R., Reyes-Villegas, E., Spracklen, D. V., Reddington, C. L., Kong, S. F., Williams, P. I., Ting, Y. C., Haslett, S., Taylor, J. W., Flynn, M. J., Morgan, W. T., McFiggans, G., Coe, H., and Allan, J. D.: Black-carbon absorption enhancement in the atmosphere determined by particle mixing state, *Nature Geoscience*, 10, 184–U132, <GotoISI>://WOS:000395791400009, 2017.
- 25 Liu, L. and Mishchenko, M. I.: Effects of aggregation on scattering and radiative properties of soot aerosols, *Journal of Geophysical Research-Atmospheres*, 110, <GotoISI>://WOS:000229988800009, 2005.
- Liu, X., Easter, R. C., Ghan, S. J., Zaveri, R., Rasch, P., Shi, X., Lamarque, J. F., Gettelman, A., Morrison, H., Vitt, F., Conley, A., Park, S., Neale, R., Hannay, C., Ekman, A. M. L., Hess, P., Mahowald, N., Collins, W., Iacono, M. J., Bretherton, C. S., Flanner, M. G., and Mitchell, D.: Toward a minimal representation of aerosols in climate models: description and evaluation in the Community Atmosphere Model CAM5, *Geoscientific Model Development*, 5, 709–739, <GotoISI>://WOS:000305964700001, 2012.
- 30 Luo, J., Zhang, Y., Wang, F., Wang, J., and Zhang, Q.: Applying machine learning to estimate the optical properties of black carbon fractal aggregates, *Journal of Quantitative Spectroscopy and Radiative Transfer*, 215, 1 – 8, <https://doi.org/https://doi.org/10.1016/j.jqsrt.2018.05.002>, <https://www.sciencedirect.com/science/article/pii/S0022407317309238>, 2018a.



- Luo, J., Zhang, Y., Zhang, Q., Wang, F., Liu, J., and Wang, J.: Sensitivity analysis of morphology on radiative properties of soot aerosols, *Optics Express*, 26, A420–A432, <https://doi.org/10.1364/OE.26.00A420>, <http://www.opticsexpress.org/abstract.cfm?URI=oe-26-10-A420>, 2018b.
- Luo, J., Zhang, Y. M., and Zhang, Q. X.: A model study of aggregates composed of spherical soot monomers with an acentric carbon shell, *Journal of Quantitative Spectroscopy and Radiative Transfer*, 205, 184–195, <GotoISI>://WOS:000417665000021, 2018c.
- Ma, X., Yu, F., and Luo, G.: Aerosol direct radiative forcing based on GEOS-Chem-APM and uncertainties, *Atmospheric Chemistry and Physics*, 12, 5563–5581, <GotoISI>://WOS:000305835900016, 2012.
- Mackowski, D. W.: MSTM Version 3.0: April 2013, <http://www.eng.auburn.edu/~dmckwski/scatcodes/>, 2013.
- Mackowski, D. W. and Mishchenko, M. I.: A multiple sphere T-matrix Fortran code for use on parallel computer clusters, *Journal of Quantitative Spectroscopy and Radiative Transfer*, 112, 2182–2192, <GotoISI>://WOS:000294518300013, 2011.
- Mie, G.: Beiträge zur Optik trüber Medien, speziell kolloidaler Metallösungen, *Annalen Der Physik*, 330, 377–445, <https://doi.org/10.1002/andp.19083300302>, 1908.
- Mishchenko, M. I., Travis, L. D., and Lacis, A. A.: *Scattering, absorption, and emission of light by small particles*, Cambridge university press, 2002.
- Mishchenko, M. I., Liu, L., Travis, L. D., and Lacis, A. A.: Scattering and radiative properties of semi-external versus external mixtures of different aerosol types, *Journal of Quantitative Spectroscopy and Radiative Transfer*, 88, 139–147, <GotoISI>://WOS:000223415600015, 2004.
- Moffet, R. C. and Prather, K. A.: In-situ measurements of the mixing state and optical properties of soot with implications for radiative forcing estimates, *Proceedings of the National Academy of Sciences of the United States of America*, 106, 11 872–11 877, <GotoISI>://WOS:000268178400013, 2009.
- Moosmuller, H., Chakrabarty, R. K., and Arnott, W. P.: Aerosol light absorption and its measurement: A review, *Journal of Quantitative Spectroscopy and Radiative Transfer*, 110, 844–878, <GotoISI>://WOS:000267082200006, 2009.
- Naoe, H., Hasegawa, S., Heintzenberg, J., Okada, K., Uchiyama, A., Zaizen, Y., Kobayashi, E., and Yamazaki, A.: State of mixture of atmospheric submicrometer black carbon particles and its effect on particulate light absorption, *Atmospheric Environment*, 43, 1296–1301, <GotoISI>://WOS:000263426600016, 2009.
- Schnaiter, M., Linke, C., Mohler, O., Naumann, K. H., Saathoff, H., Wagner, R., Schurath, U., and Wehner, B.: Absorption amplification of black carbon internally mixed with secondary organic aerosol, *Journal of Geophysical Research-Atmospheres*, 110, <GotoISI>://WOS:000232553600003, 2005.
- Schwarz, J. P., Spackman, J. R., Fahey, D. W., Gao, R. S., Lohmann, U., Stier, P., Watts, L. A., Thomson, D. S., Lack, D. A., Pfister, L., Mahoney, M. J., Baumgardner, D., Wilson, J. C., and Reeves, J. M.: Coatings and their enhancement of black carbon light absorption in the tropical atmosphere, *Journal of Geophysical Research-Atmospheres*, 113, <GotoISI>://WOS:000253233700002, 2008.
- Shamjad, P. M., Satish, R. V., Thamban, N. M., Rastogi, N., and Tripathi, S. N.: Absorbing Refractive Index and Direct Radiative Forcing of Atmospheric Brown Carbon over Gangetic Plain, *Acs Earth and Space Chemistry*, 2, 31–37, <GotoISI>://WOS:000423141600004, 2018.
- Smith, D. A. and Stokes, K. L.: Discrete dipole approximation for magneto-optical scattering calculations, *Optics Express*, 14, 5746–5754, <GotoISI>://WOS:000238437800090, 2006.
- Sorensen, C. M.: Light scattering by fractal aggregates: A review, *Aerosol Science and Technology*, 35, 648–687, <GotoISI>://WOS:000170467100003, 2001.



- Sorensen, C. M. and Roberts, G. C.: The prefactor of fractal aggregates, *Journal of Colloid and Interface Science*, 186, 447–452, <GotoISI>://WOS:A1997WK06000026, 1997.
- Strawa, A. W., Drdla, K., Ferry, G. V., Verma, S., Pueschel, R. F., Yasuda, M., Salawitch, R. J., Gao, R. S., Howard, S. D., Bui, P. T., Loewenstein, M., Elkins, J. W., Perkins, K. K., and Cohen, R.: Carbonaceous aerosol (Soot) measured in the lower stratosphere during POLARIS and its role in stratospheric photochemistry, *Journal of Geophysical Research-Atmospheres*, 104, 26 753–26 766, <GotoISI>://WOS:000083781200045, 1999.
- Taflove, A. and Hagness, S. C.: *Computational electrodynamics: the finite-difference time-domain method*, Artech house, 2005.
- Thouy, R. and Jullien, R.: A Cluster-Cluster Aggregation Model with Tunable Fractal Dimension, *Journal of Physics a-Mathematical and General*, 27, 2953–2963, <GotoISI>://WOS:A1994NM53200012, 1994.
- 10 Wang, Q. Y., Huang, R. J., Cao, J. J., Tie, X. X., Ni, H. Y., Zhou, Y. Q., Han, Y. M., Hu, T. F., Zhu, C. S., Feng, T., Li, N., and Li, J. D.: Black carbon aerosol in winter northeastern Qinghai-Tibetan Plateau, China: the source, mixing state and optical property, *Atmospheric Chemistry and Physics*, 15, 13 059–13 069, <GotoISI>://WOS:000365977100021, 2015.
- Wentzel, M., Gorzawski, H., Naumann, K. H., Saathoff, H., and Weinbruch, S.: Transmission electron microscopical and aerosol dynamical characterization of soot aerosols, *Journal of Aerosol Science*, 34, 1347–1370, <GotoISI>://WOS:000185856300004, 2003.
- 15 Woźniak, M.: *Characterization of nanoparticle aggregates with light scattering techniques*, Thesis, 2012.
- Wu, Y., Cheng, T. H., Gu, X. F., Zheng, L. J., Chen, H., and Xu, H.: The single scattering properties of soot aggregates with concentric core-shell spherical monomers, *Journal of Quantitative Spectroscopy and Radiative Transfer*, 135, 9–19, <GotoISI>://WOS:000331680400002, 2014.
- Xu, Y. L.: Calculation of the addition coefficients in electromagnetic multisphere-scattering theory (vol 127, pg 285, 1996), *Journal of Computational Physics*, 134, 200–200, <GotoISI>://WOS:A1997XC98800014, 1997.
- 20 Xu, Y. L. and Gustafson, B. A. S.: A generalized multiparticle Mie-solution: further experimental verification, *Journal of Quantitative Spectroscopy and Radiative Transfer*, 70, 395–419, <GotoISI>://WOS:000169975700004, 2001.
- Xue, H. X., Khalizov, A. F., Wang, L., Zheng, J., and Zhang, R. Y.: Effects of dicarboxylic acid coating on the optical properties of soot, *Physical Chemistry Chemical Physics*, 11, 7869–7875, <GotoISI>://WOS:000269548300013, 2009.
- 25 Yang, P., Wei, H. L., Kattawar, G. W., Hu, Y. X., Winker, D. M., Hostetler, C. A., and Baum, B. A.: Sensitivity of the backscattering Mueller matrix to particle shape and thermodynamic phase, *Applied Optics*, 42, 4389–4395, <GotoISI>://WOS:000184252300020, 2003.
- Yee, K.: Numerical solution of initial boundary value problems involving Maxwell's equations in isotropic media, *IEEE Transactions on antennas and propagation*, 14, 302–307, 1966.
- You, R., Radney, J. G., Zachariah, M. R., and Zangmeister, C. D.: Measured Wavelength-Dependent Absorption Enhancement of Internally Mixed Black Carbon with Absorbing and Nonabsorbing Materials, *Environmental Science and Technology*, 50, 7982–7990, <GotoISI>://WOS:000381063200006, 2016.
- 30 Zhang, R. Y., Khalizov, A. F., Pagels, J., Zhang, D., Xue, H. X., and McMurry, P. H.: Variability in morphology, hygroscopicity, and optical properties of soot aerosols during atmospheric processing, *Proceedings of the National Academy of Sciences of the United States of America*, 105, 10 291–10 296, <GotoISI>://WOS:000258211600006, 2008.
- 35 Zhang, X. L., Mao, M., Yin, Y., and Wang, B.: Absorption enhancement of aged black carbon aerosols affected by their microphysics: A numerical investigation, *Journal of Quantitative Spectroscopy and Radiative Transfer*, 202, 90–97, <GotoISI>://WOS:000412962100014, 2017.



Zhang, X. L., Mao, M., Yin, Y., and Wang, B.: Numerical Investigation on Absorption Enhancement of Black Carbon Aerosols Partially Coated With Nonabsorbing Organics, *Journal of Geophysical Research-Atmospheres*, 123, 1297–1308, <GotoISI>://WOS:000425520200039, 2018.



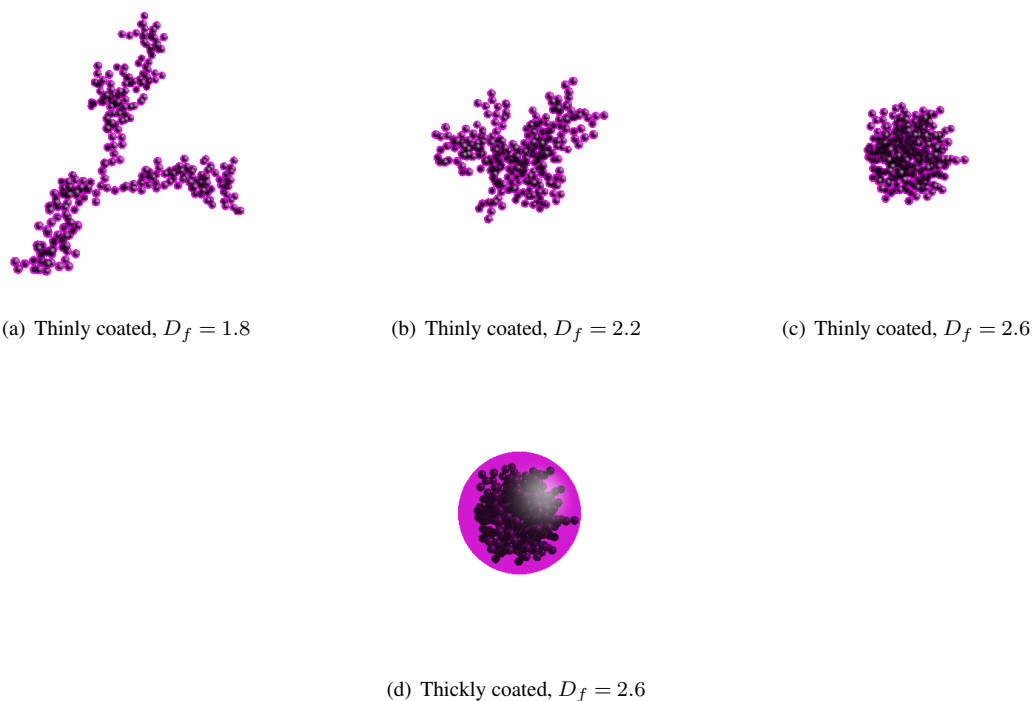


**Figure 1.** Typical morphologies of BC,  $n_s = 300$ ,  $k_0 = 1.2$ .

**Table 1.** Morphological parameters of BC aerosols

Parameters	Thinly-coated BC	Thickly-coated BC
$k_o$	1.2	1.2
$n_s$	1-1000	1-1000
$D_f$	1.8,2.2,2.6	2.6
$f_{soot}$	0.2,0.4,0.6,0.8,1.0	0.05, 0.06, 0.075, 0.1

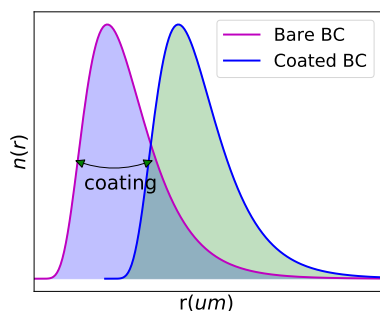


**Figure 2.** Size distribution of bare and coated BC.

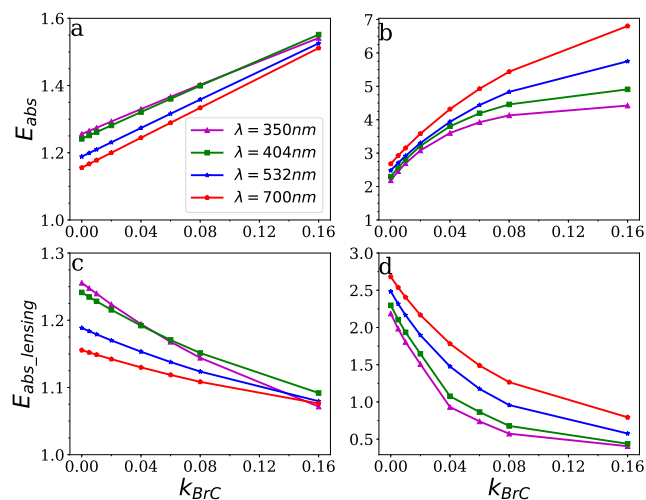


**Figure 3.** Effects of  $K_{BrC}$  on lensing effects and absorption enhancement ( $n_s = 200$ ). (a) Absorption enhancements of thinly-coated BC ( $D_f = 2.2$ ,  $f_{BC} = 40\%$ ); (b) Absorption enhancements of thickly-coated BC ( $D_f = 2.6$ ,  $f_{BC} = 5\%$ ); (c) same as (a) but for lensing effects; (d) same as (b) but for lensing effects.

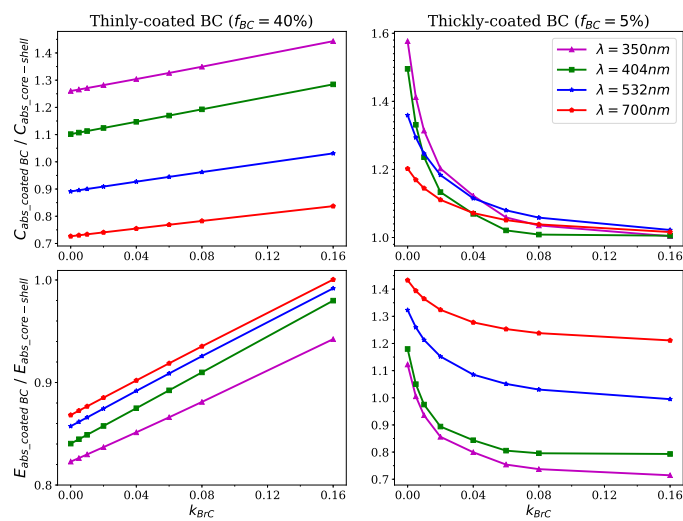


**Figure 4.** Effects of  $k_{BrC}$  on the applicability of core-shell sphere ( $n_s = 200$ ).

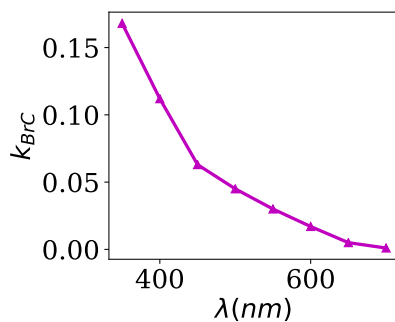


**Figure 5.** Imaginary part of the refractive index of BrC based on the study of Kirchstetter et al. (2004).

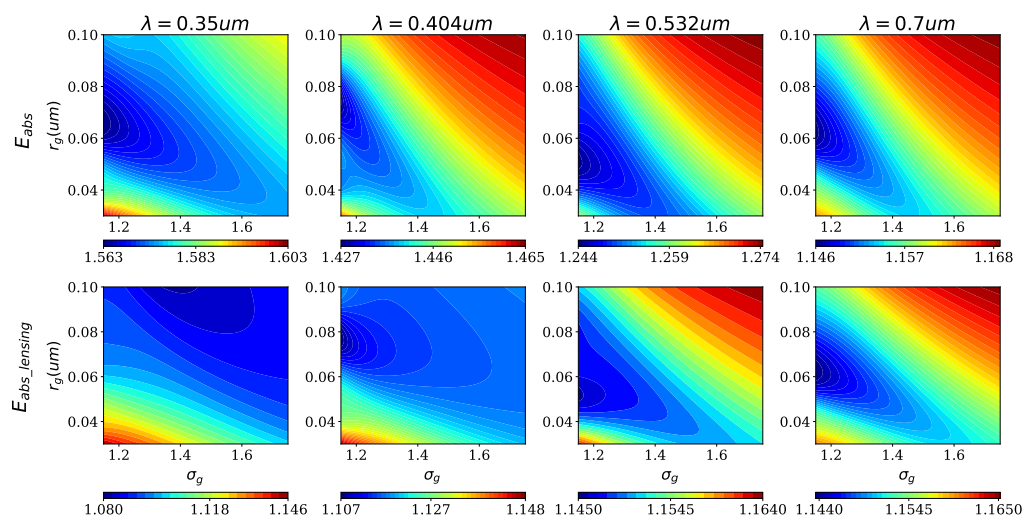


**Figure 6.**  $E_{abs}$  and  $E_{abs,lensing}$  of thinly-coated BC with BrC coatings at different size distributions ( $D_f = 2.2$ ,  $f_{BC} = 40\%$ ).

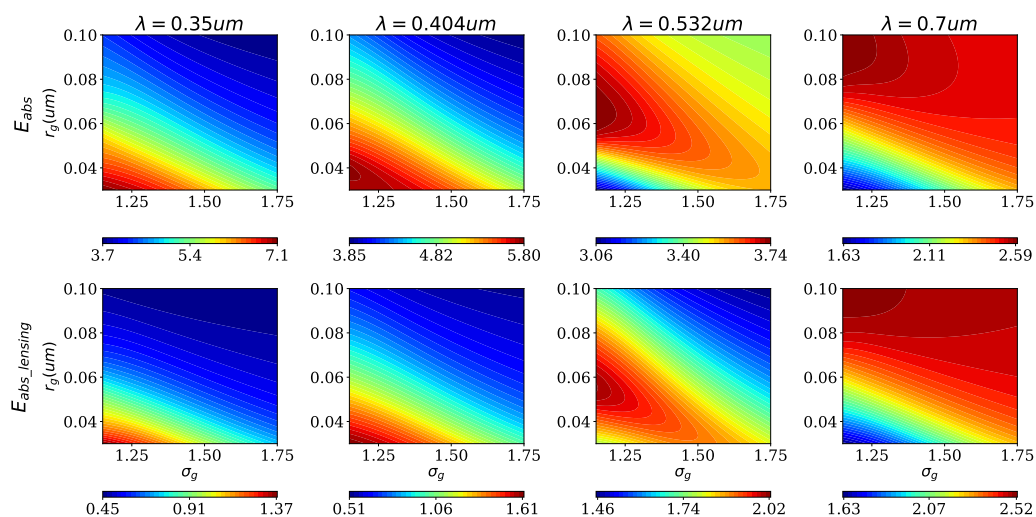


**Figure 7.**  $E_{abs}$  and  $E_{abs,lensing}$  of thickly-coated BC with BrC at different size distributions ( $D_f = 2.6$ ,  $f_{BC} = 6\%$ ).

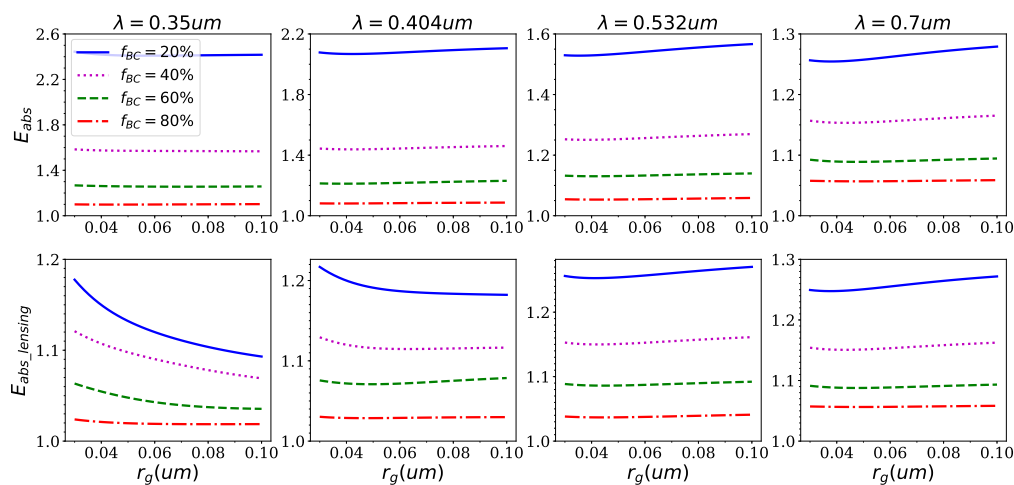


**Figure 8.**  $E_{abs}$  and  $E_{abs\_lensing}$  of thinly-coated BC with BrC varying with  $r_g$  at different  $f_{BC}$  ( $D_f = 2.2$ ,  $\sigma_g = 1.5$ ).

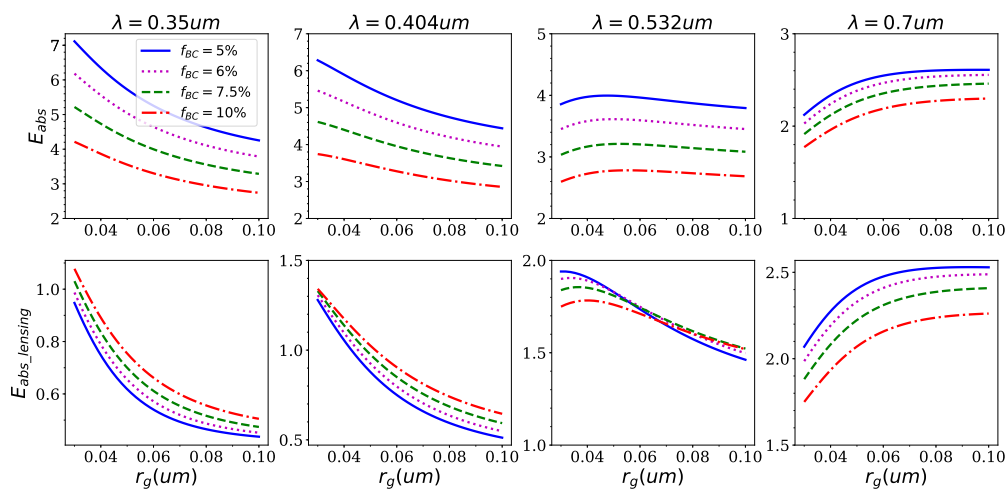


**Figure 9.**  $E_{abs}$  and  $E_{abs\_lensing}$  of thickly-coated BC with BrC varying with  $r_g$  at different  $f_{BC}$  ( $D_f = 2.6$ ,  $\sigma_g = 1.5$ ).

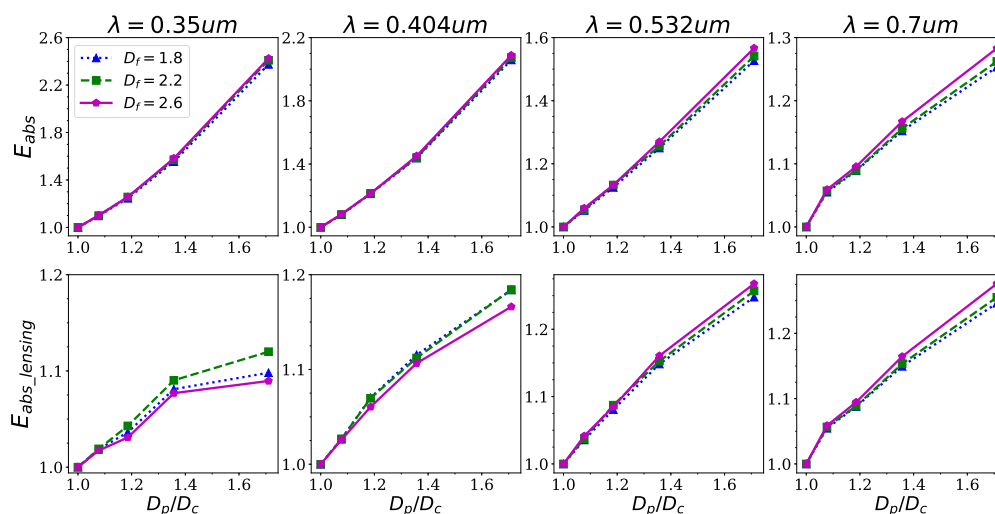


**Figure 10.**  $E_{abs}$  and  $E_{abs\_lensing}$  of thinly-coated BC with BrC coatings varying with  $D_p/D_c$  for different  $D_f$  ( $r_g = 0.06\mu m$ ,  $\sigma_g = 1.5$ ).

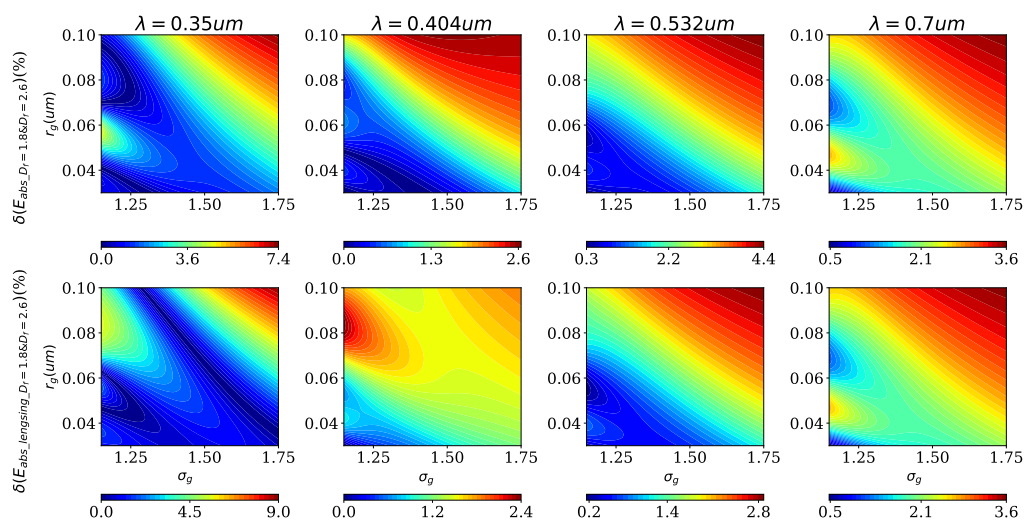


**Figure 11.** The relative deviations of absorption properties between  $D_f = 1.8$  and  $D_f = 2.6$  for thinly-coated BC with BrC coating ( $f_{BC} = 20\%$ ).



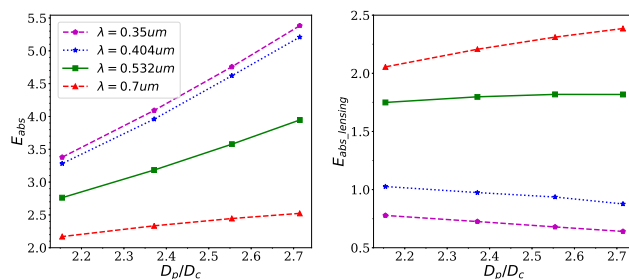


**Figure 12.**  $E_{abs}$  and  $E_{abs\_lensing}$  of thickly-coated BC with BrC coating varying with  $D_p/D_c$  for different  $\lambda$  ( $D_f = 2.6$ ,  $r_g = 0.06 \mu m$ ,  $\sigma_g = 1.5$ ).

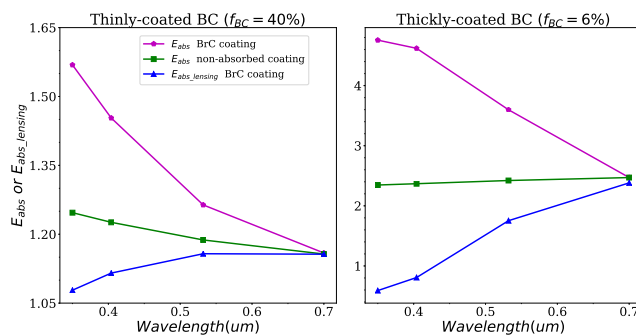


**Figure 13.** Comparison of BC coated with non-absorbing materials and that coated with BrC ( $r_g = 0.06 \mu m$ ,  $\sigma_g = 1.5$ ).  $D_f = 2.2$  and  $D_f = 2.6$  were assumed for thinly-coated and thickly-coated BC, respectively.